Available online at www.sciencedirect.com
SCIENCE DIRECT
Journal of Sound and Vibration 294 (2006) 624–636
JOURNAL OF SOUND AND VIBRATION
www.elsevier.com/locate/jsvi

Short Communication

Subharmonic resonances of a mechanical oscillator with periodically time-varying, piecewise-nonlinear stiffness

Qinglong Ma, A. Kahraman*

Department of Mechanical Engineering, The Ohio State University, Columbus, 206 W. 18th Avenue, OH 43210, USA

Received 21 January 2005; received in revised form 28 October 2005; accepted 29 November 2005
Available online 17 February 2006

Abstract

The subharmonic (period-η, $\eta > 1$) motions of a piecewise-nonlinear (PN) mechanical oscillator having parametric and external excitations are investigated. The system is formed by a viscously damped, single-degree-of-freedom oscillator subjected to a periodically time-varying, PN stiffness defined by a clearance surrounded by continuous forms of nonlinearity. A multiterm harmonic balance formulation in conjunction with discrete Fourier transforms is used to determine steady-state period-η motions of the system near the parametric instability regions. The accuracy of analytical solutions is verified through a comparison with direct numerical integration results. A parametric study is also presented to demonstrate the combined influence of a clearance and of cubic nonlinearities on period-η motions within typical ranges of system and excitation parameters.

1. Introduction

The subharmonic resonance of a single-degree-of-freedom (sdof) piecewise-nonlinear (PN) oscillator is investigated in this paper. The equation of motion is given in dimensionless form as

$$\ddot{u}(\tau) + 2\zeta\dot{u}(\tau) + w(\tau)g[u(\tau)] = f(\tau), \tag{1}$$

where τ is dimensionless time, an overdot denotes differentiation with respect to τ, $u(\tau)$ is displacement response of a unit mass, and ζ is the viscous damping ratio. The restoring function $g[u(\tau)]$ is considered to be a PN function, and a special case is used in this study as

$$g[u(\tau)] = \begin{cases} \sum_{i=1}^{3} \alpha_i [u(\tau) - 1]^i & u(\tau) > 1, \\ 0 & -1 \leqslant u(\tau) \leqslant 1, \\ \sum_{i=1}^{3} (-1)^{i-1} \alpha_i [u(\tau) + 1]^i & u(\tau) < -1. \end{cases} \tag{2}$$

*Corresponding author. Tel.: +1 614 292 4678; fax: +1 614 292 3136.
E-mail address: kahraman.1@osu.edu (A. Kahraman).

0022-460X/$ - see front matter © 2006 Elsevier Ltd. All rights reserved.
doi:10.1016/j.jsv.2005.11.026

In addition, Eq. (1) includes an external periodic excitation $f(\tau)$ and an internal parametric excitation $w(\tau)$. Period-1 motions of the same nonlinear oscillator were investigated in a recent paper by these authors [1] using a multiterm harmonic balance method (HBM). The results were shown to agree well with numerical solutions. A parametric study was provided to demonstrate the combined effects of significant system parameters and continuous nonlinearities of $g[u(\tau)]$ on period-1 motions of the system. Meanwhile, mechanical systems having $g[u(\tau)]$ as in Eq. (2) are expected to exhibit subharmonic and chaotic motions as well. In previous studies, Choi and Noah [2] examined the subharmonic response of a sdof time-invariant bilinear system by using HBM. Later, Choi and Lou [3] determined the forced steady-state response of a system with unsymmetric time-invariant PN stiffness by an improved HBM algorithm that incorporates fast Fourier transforms. Kahraman and Blankenship [4,5] demonstrated the existence of period-2, subharmonic resonances through measurements from a spur gear pair. They also predicted the subharmonic response analytically by using a piecewise-linear (PL) version of $g[u(\tau)]$ with $\alpha_2 = \alpha_3 = 0$. Recently, Al-shyyab and Kahraman [6] predicted period-η and chaotic motions using a PL dynamic model of a multimesh gear system. However, these studies were limited to either a PN version of $g[u(\tau)]$ with no parametric excitation [3], or a PL version with or without parametric excitation [2,4–6].

In this paper, the formulation presented in reference [1] is extended to predict period-η subharmonic motions exhibited by Eq. (1). The same multiterm HBM is used in conjunction with discrete Fourier transforms (DFT) to obtain steady-state period-η response. The accuracy of HBM solutions is demonstrated through a comparison with numerical integration results. The results of a parametric study are presented to describe the combined influence of continuous nonlinearities and clearance on the steady-state response of the PN system defined by Eq. (1). In addition, the effect of system parameters, such as ζ, $w(\tau)$, preload f_1, and $f(\tau)$, on period-η motions is investigated.

2. Period-η response to periodic excitations

The multiterm HBM formulation presented in Ref. [1] for period-1 motions is modified here to predict period-η ($\eta \geqslant 1$) motions of the same system. First, the periodic excitations $w(\tau)$ and $f(\tau)$ are given in Fourier series form as

$$w(\tau) = w_1 + \sum_{\kappa=1}^{K} [w_{2\kappa} \cos(\kappa \Lambda \tau) + w_{2\kappa+1} \sin(\kappa \Lambda \tau)], \tag{3a}$$

$$f(\tau) = f_1 + \sum_{\mu=1}^{M} [f_{2\mu} \cos(\mu \Lambda \tau) + f_{2\mu+1} \sin(\mu \Lambda \tau)]. \tag{3b}$$

Next, a new independent variable is defined as $\theta = \Lambda\tau/\eta$, and $H = \Lambda/\eta$, where η is the sub-harmonic index. The unknown steady state, period-η response $u(\theta)$ and the nonlinear restoring function $g[u(\theta)]$ are also assumed to be periodic and expressed in Fourier series as

$$u(\theta) = u_1 + \sum_{r=1}^{\eta R} [u_{2r} \cos(r\theta) + u_{2r+1} \sin(r\theta)], \tag{4a}$$

$$g[u(\theta)] = v_1 + \sum_{r=1}^{\eta R} [v_{2r} \cos(r\theta) + v_{2r+1} \sin(r\theta)]. \tag{4b}$$

Substituting these equation into the equation of motion and enforcing harmonic balance yield a vector equation $\mathbf{S} = \mathbf{0}$, where $\mathbf{S} = [S_1 S_2 S_3, \ldots, S_{2\eta R} S_{2\eta R+1}]^{\mathrm{T}}$, and

$$S_1 = v_1 - f_1 + \frac{1}{2} \sum_{k=1}^{K} [w_{2k} v_{2k\eta} + w_{2k+1} v_{2k\eta+1}], \tag{5a}$$

$$S_{2r} = -H^2r^2u_{2r} + 2\zeta Hru_{2r+1} + v_{2r} + v_1w_{2r/\eta} - f_{2r/\eta} + \frac{1}{2}\sum_{k=1}^{K} w_{2k}[v_{2(k\eta-r)} + v_{2(k\eta+r)} + v_{2(r-k\eta)}] + \frac{1}{2}\sum_{k=1}^{K} w_{2k+1}[v_{2(k\eta-r)+1} + v_{2(k\eta+r)+1} - v_{2(r-k\eta)+1}], \quad r \in [1, \eta R], \tag{5b}$$

$$S_{2r+1} = -H^2r^2u_{2r+1} - 2\zeta Hru_{2r} + v_{2r+1} + v_1w_{(2r/\eta)+1} - f_{(2r/\eta)+1} + \frac{1}{2}\sum_{k=1}^{K} w_{2k}[-v_{2(k\eta-r)+1} + v_{2(k\eta+r)+1} + v_{2(r-k\eta)+1}] + \frac{1}{2}\sum_{k=1}^{K} w_{2k+1}[v_{2(k\eta-r)} - v_{2(k\eta+r)} + v_{2(r-k\eta)}], \quad r \in [1, \eta R], \tag{5c}$$

Here, the Fourier coefficients v_{2r} and v_{2r+1} of $g[u(\theta)]$ are calculated by employing DFT as described in Ref. [1]. Hence, the above $2\eta R+1$ algebraic equations $\mathbf{S}=\mathbf{0}$ are solved for $2\eta R+1$ unknowns u_i by using the Newton–Raphson method as

$$\mathbf{u}^{(m)} = \mathbf{u}^{(m-1)} - [\mathbf{J}^{-1}]^{(m-1)}\mathbf{S}^{(m-1)}, \tag{6}$$

where $\mathbf{u} = [u_1u_2u_3, \ldots, u_{2\eta R}u_{2\eta R+1}]^{\mathrm{T}}$, and m is the iteration index. The stability of the steady-state response is determined by using Floquet theory [1].

3. Results

3.1. Comparison to direct numerical integration results

In order to evaluate the accuracy of HBM solutions from Eqs. (5) and (6), Eq. (1) is integrated numerically utilizing a variable-order backward differentiation formula. An example of a periodic $w(\tau)$ ($w_2 = 0.4$, $w_4 = 0.15$, $w_6 = 0.05$, $K = 3$, and all other $w_i = 0$) is considered here. This approximates the mesh stiffness of an unmodified spur gear pair with an involute contact ratio of 1.37 [7]. The external force is assumed to be constant with $f_1 = 0.5$ and $f_i = 0 (i > 1)$. Moreover, $\zeta = 0.01$, and $g[u(\tau)]$ contains linear, quadratic, and cubic terms with $\alpha_1 = 1$, $\alpha_2 = 0.1$, and $\alpha_3 = 0.2$, respectively.

In Fig. 1(a), the root-mean-square (RMS) amplitudes of both stable and unstable period-η ($\eta = 1, 2, 3$) HBM solutions are shown as a function of Λ. These solutions are obtained by solving Eq. (1) for different η separately. To estimate period-η solutions, 6η harmonic terms ($R = 6$) are assumed. The RMS value of the response is defined as $u^{\eta}_{\mathrm{rms}} = \left[\sum_{r=1}^{\eta R}(u_{2r}^2 + u_{2r+1}^2)\right]^{1/2}$. A good agreement is observed between the HBM and numerical solutions. Period-2 motions emerge when period-1 motions become unstable near the first parametric resonance frequency of $\Lambda = 2$. Stable period-1 and period-2 motions coexist for $\Lambda \in (1.38, 1.93)$, while only period-2 motions are present when $\Lambda \in (1.93, 2.45)$. The shape of the period-2 resonance peak is similar to that of a typical primary resonance of period-1 motions near $\Lambda = 1$ with a pair of softening branches (one stable and one unstable) bent to the left due to contact loss (single-sided impacts (SSI)) followed by another pair of hardening branches owing to back contact (double-sided impacts (DSI)). A period-3 subharmonic resonance exists in Fig. 1(a) near $\Lambda = 3$. Similar to PL systems as in Ref. [5], a "boomerang-shaped" island arises, which is entirely isolated from the stable period-1 motions below. Similarly, a comparison of the mean component of system response u_1 from the HBM and numerical integration is shown in Fig. 1(b), which further illustrates the agreement between two methods. While the results from the HBM and numerical integration method agree satisfactorily in Fig. 1, more numerical solutions should be expected, especially on the hardening portions of the primary and subharmonic resonance peaks. A main difficulty is that the numerical integration method is inefficient in terms of computation time, particularly for lightly damped systems. In addition, in the regions where multiple stable solutions coexist, one needs to search for

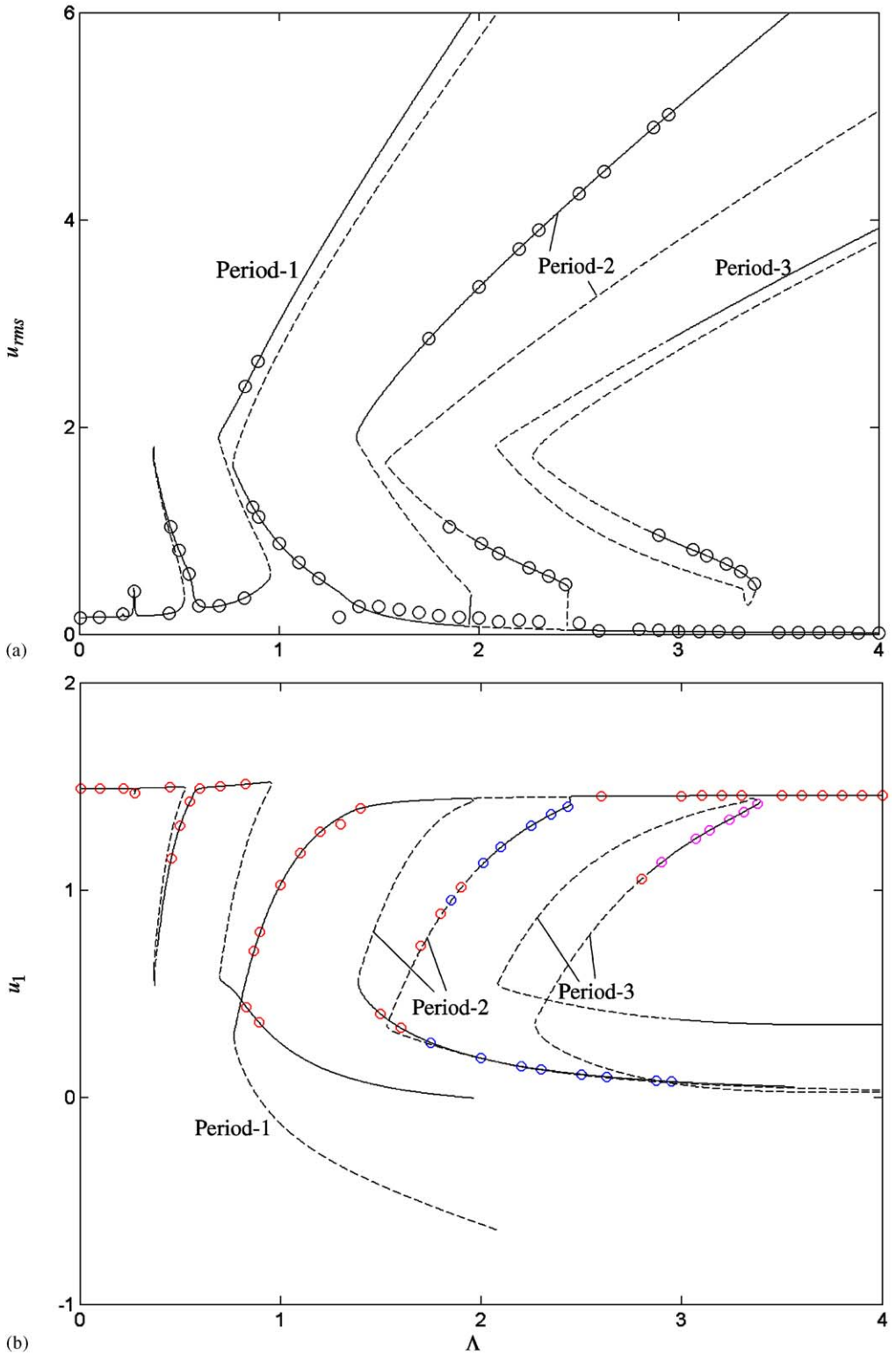

Fig. 1. (a) u_{rms} and (b) u_1 values of period-η ($\eta = 1, 2$, and 3) motions ($R = 6$) as a function of Λ given $\alpha_2 = 0.1$, $\alpha_3 = 0.2$, $f_1 = 0.5$, $f_i = 0$ ($i \geqslant 2$), $w_2 = 0.4$, $w_4 = 0.15$, $w_6 = 0.05$ ($K = 3$), all other $w_i = 0$, and $\zeta = 0.01$. (—) stable HBM solutions, (– –) unstable HBM solutions, and (○) numerical integration solutions.

proper initial conditions by trial-and-error to obtain the desired steady-state solutions. As a result, the numerical solutions presented in Fig. 1 are incomplete, while HBM solutions are not subject to such difficulties.

3.2. Parametric studies

A parameter set of $[\alpha_1, \alpha_2, \alpha_3, f_1, f_i, w_i, \zeta, \Lambda]$ is considered for investigating the dynamic behavior of the systems governed by Eq. (1). In Ref. [1], the influence of this set on period-1 motions was studied in detail for $\Lambda \in [0, 1.5]$. In this section, period-η motions within a wider range of $\Lambda \in [0, 6]$ are investigated. In order to limit the parametric study to a reasonable size, only period-2 and period-3 motions are considered, but the formulation can handle higher subharmonic motions as well. The maximum harmonic index of the Fourier series is chosen as $R = 6$, which results in sufficiently accurate period-1 solutions as shown in Fig. 1. Therefore, the numbers of harmonic terms for period-2 and period-3 motions are chosen as $\eta R = 12$ and 18 terms, correspondingly. The RMS value of the response u_{rms} is utilized to represent $u(\tau)$. In the figures provided in the following sections, solid and dashed lines represent stable and unstable motions, respectively.

In Figs. 2 and 3, the effect of the cubic nonlinear term α_3 on period-2 and period-3 motions is shown. In this case, quadratic nonlinearity is not included, $\alpha_2 = 0$. One softening condition with $\alpha_3 = -0.1$, and two hardening conditions with $\alpha_3 = 0.2$ and 0.5, are considered in addition to the PL case of $\alpha_3 = 0$. Period-2 and period-3 motions of the PL system agree well with the results of Kahraman and Blankenship [5]. In Fig. 2, the effect of α_3 on the u_1 and u_{rms} values of period-2 parametric resonance is illustrated. For the softening case, the RMS amplitude of the resonance peak is reduced with an increment of α_3, and the resonance frequency range is shifted to the left slightly. The SSI branch bends to the left further, and there are DSI motions for $\alpha_3 = -0.1$. However, for the hardening cases, the peak of the period-2 resonance moves to the right on the frequency axis with the increment of α_3. A pair of softening type SSI response curves (one stable and one unstable) is followed by a pair of hardening type DSI curves bending to the right. The stable SSI motions bifurcate into unstable DSI motions at certain transition frequencies, while unstable SSI motions turn into stable DSI motions. The frequency of this transition increases with the value of α_3 as shown in Fig. 2. Therefore, the influence of α_3 on the period-2 response is similar to that on period-1 motions near primary resonance [1].

As in the case of PL systems [5], period-3 response represented in Fig. 3 by the RMS and mean components is mostly an isolated closed curve, and another stable branch of period-1 motions coexists at a lower amplitude that is not shown here. This period-3 resonance is associated with the second parametric resonance peak of the corresponding linear time-varying system near $\Lambda = 3$. Similar to Fig. 2, the curves of period-3 motions also move to the left when $\alpha_3 < 0$, and to the right when $\alpha_3 > 0$. For softening cases, DSI motions do not exist, while a wide range of DSI motions exists for the hardening cases. Since the upper DSI branch is completely stable for $\alpha_3 = 0$, a portion of it becomes unstable for $\alpha_3 > 0$. Numerical integration solutions indicate that higher-order subharmonic motions such as period-6 motions exist at these frequencies of unstable DSI motions. The frequency range of these unstable upper branch DSI motions is expanded by increasing α_3. As shown in Fig. 3, DSI motions are unstable when $\Lambda \in [2.08, 2.31]$ for $\alpha_3 = 0.2$, and when $\Lambda \in [2.19, 2.92]$ for $\alpha_3 = 0.5$. Moreover, unlike the period-2 motions in Fig. 2, the value of α_3 affects how low the u_{rms} of period-3 motions can get. For $\alpha_3 < 0$, increasing the magnitude of α_3 causes the response curve of period-3 motions to shrink and eventually disappear. For $\alpha_3 > 0$, a larger α_3 makes the SSI portion of the closed curve approach the stable branch of period-1 motions underneath. The effect of α_2 on period-2 and period-3 motions is similar to that of α_3, especially for hardening cases [8]. Therefore, only the influence of cubic nonlinear term α_3 on subharmonic resonance is illustrated here.

The effect of damping ratio ζ on period-2 and period-3 motions is illustrated in Fig. 4 for PN systems with $f_1 = 0.5$, $f_i = 0$ $(i \geqslant 2)$, $w_3 = 0.3$, $\alpha_1 = 1$, $\alpha_3 = 0.2$, and $\alpha_2 = 0$. In Fig. 4, both SSI and DSI type period-2 motions coexist in addition to period-1 motions that are not shown here. When ζ is as low as 0.01, these two types of motions are connected at saddle-node bifurcation points. Increasing ζ cannot eliminate the DSI motions, but makes them separate from the SSI motions. The SSI type period-2 motions disappear for $\zeta > 0.075$, and the amplitudes of the DSI motions increase significantly. Similarly, for period-3 motions, both

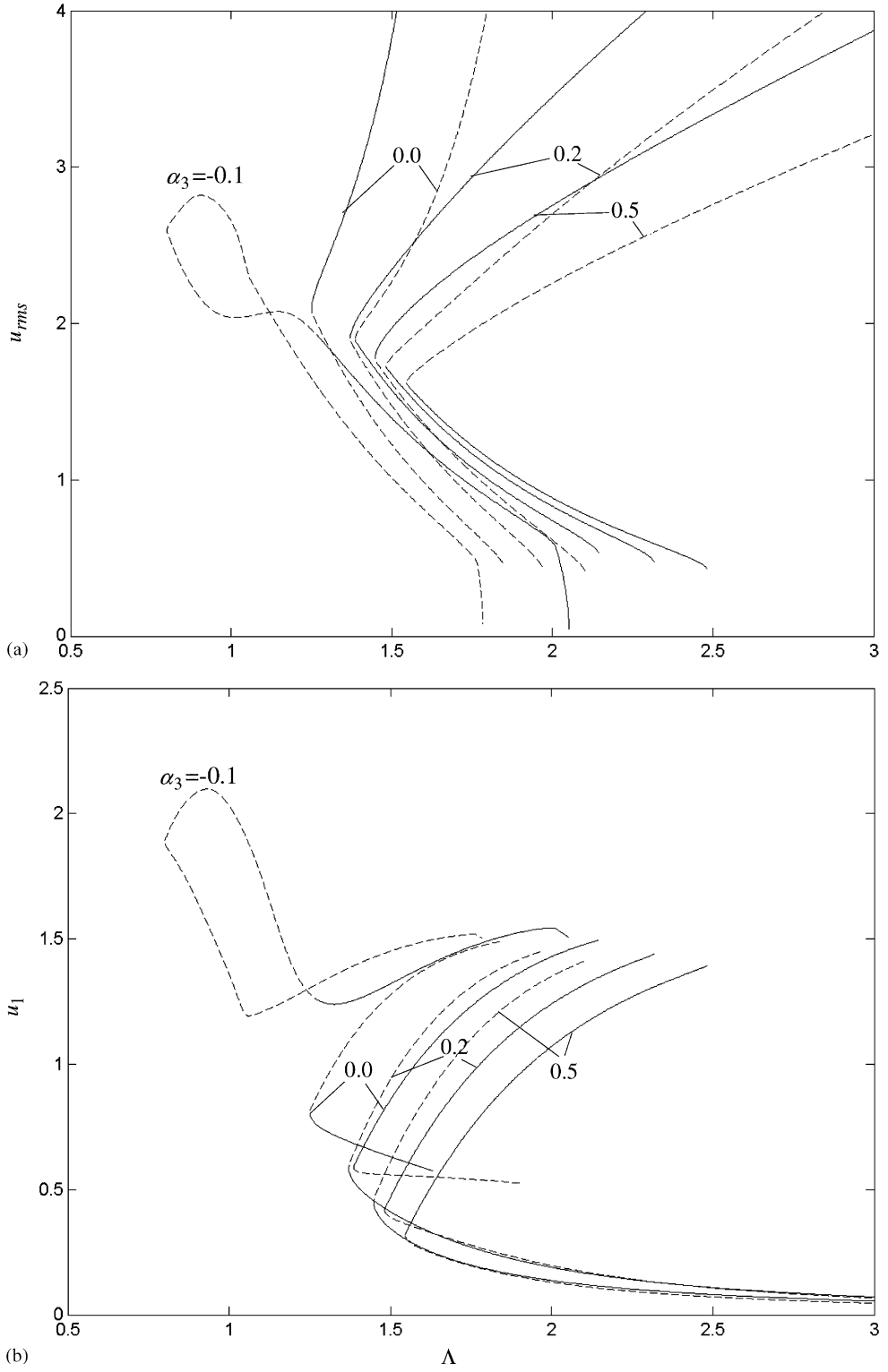

Fig. 2. Influence of α_3 on u_{rms} of an oscillator with $\alpha_1 = 1$ and $\alpha_2 = 0$, given $\zeta = 0.01, f_1 = 0.5, f_i = 0$ $(i \geqslant 2)$, $w_3 = 0.3$: (a) u_{rms} and (b) u_1 values of period-2 motions. (—) Stable and (– –) unstable HBM solutions.

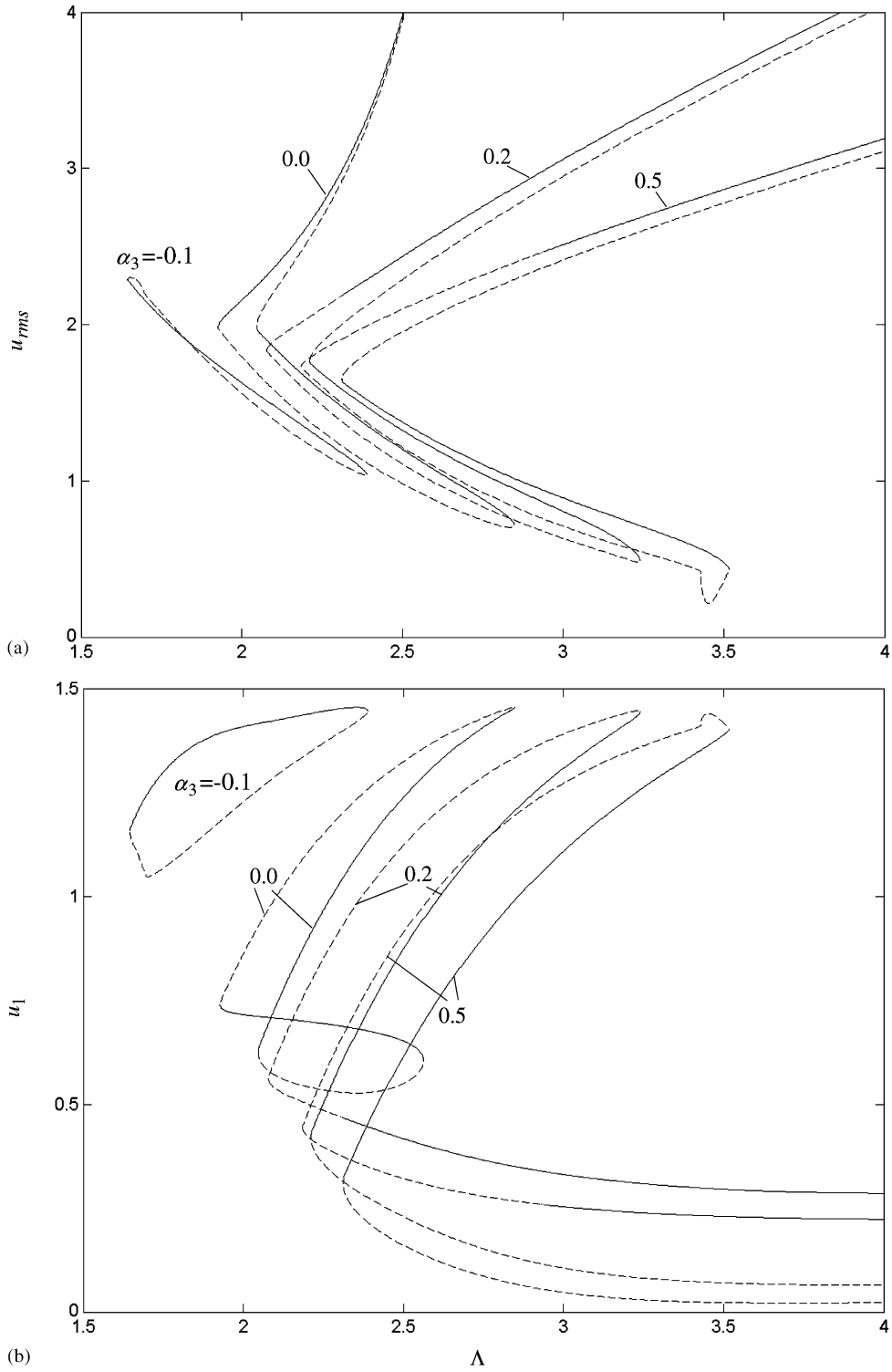

Fig. 3. Influence of α_3 on u_{rms} of an oscillator with $\alpha_1 = 1$ and $\alpha_2 = 0$, given $\zeta = 0.01, f_1 = 0.5, f_i = 0$ $(i \geqslant 2)$, $w_3 = 0.3$: (a) u_{rms} and (b) u_1 values of period-3 motions. (—) Stable and (– –) unstable HBM solutions.

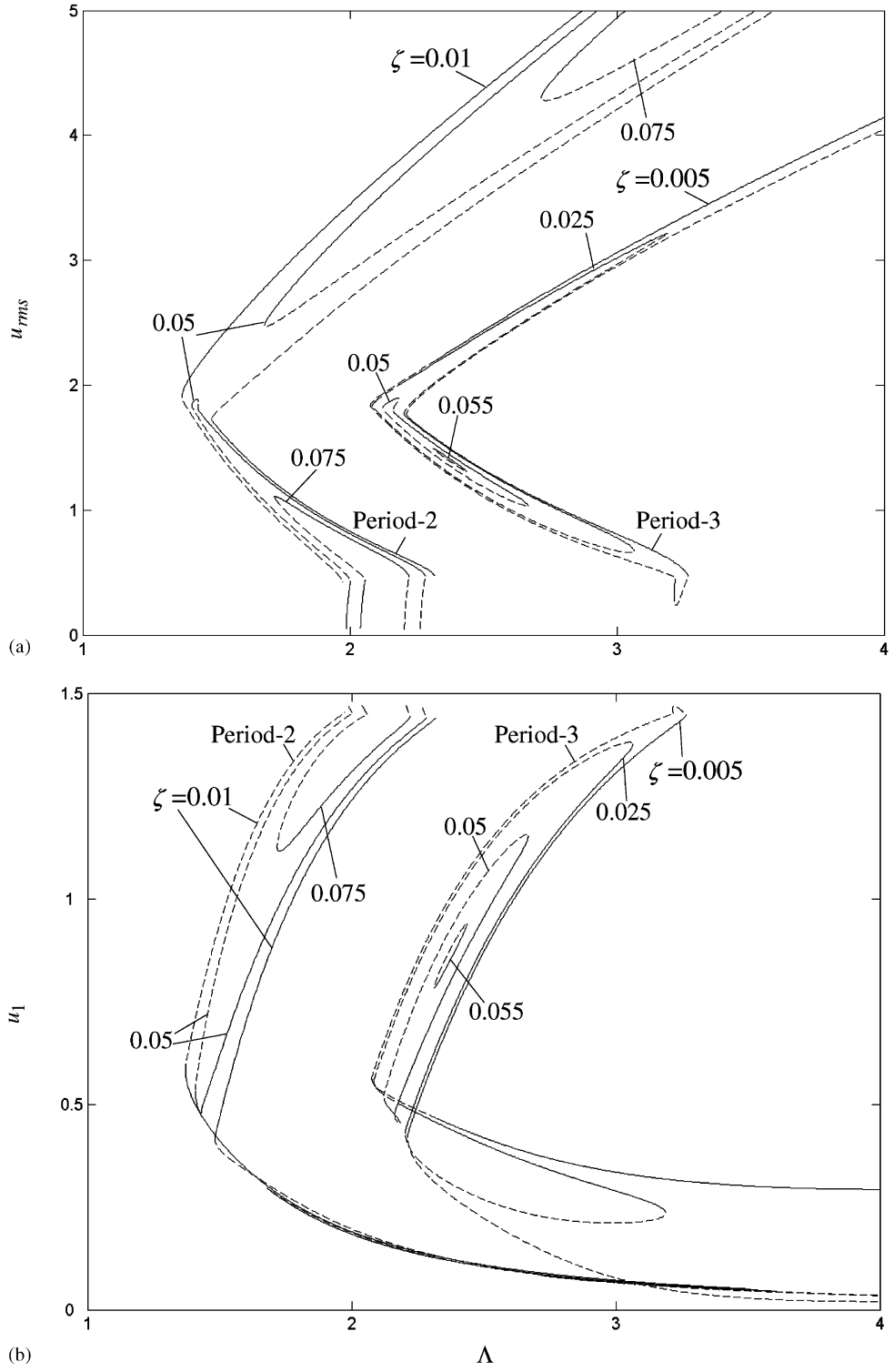

Fig. 4. Influence of ζ on u_{rms} of an oscillator with $\alpha_1 = 1$, $\alpha_2 = 0$ and $\alpha_3 = 0.2$, given $f_1 = 0.5$, $f_0 = 0$ ($i \geqslant 2$), $w_3 = 0.3$: (a) u_{rms} and (b) u_1 values of period-2 and period-3 motions. (—) Stable and (– –) unstable HBM solutions.

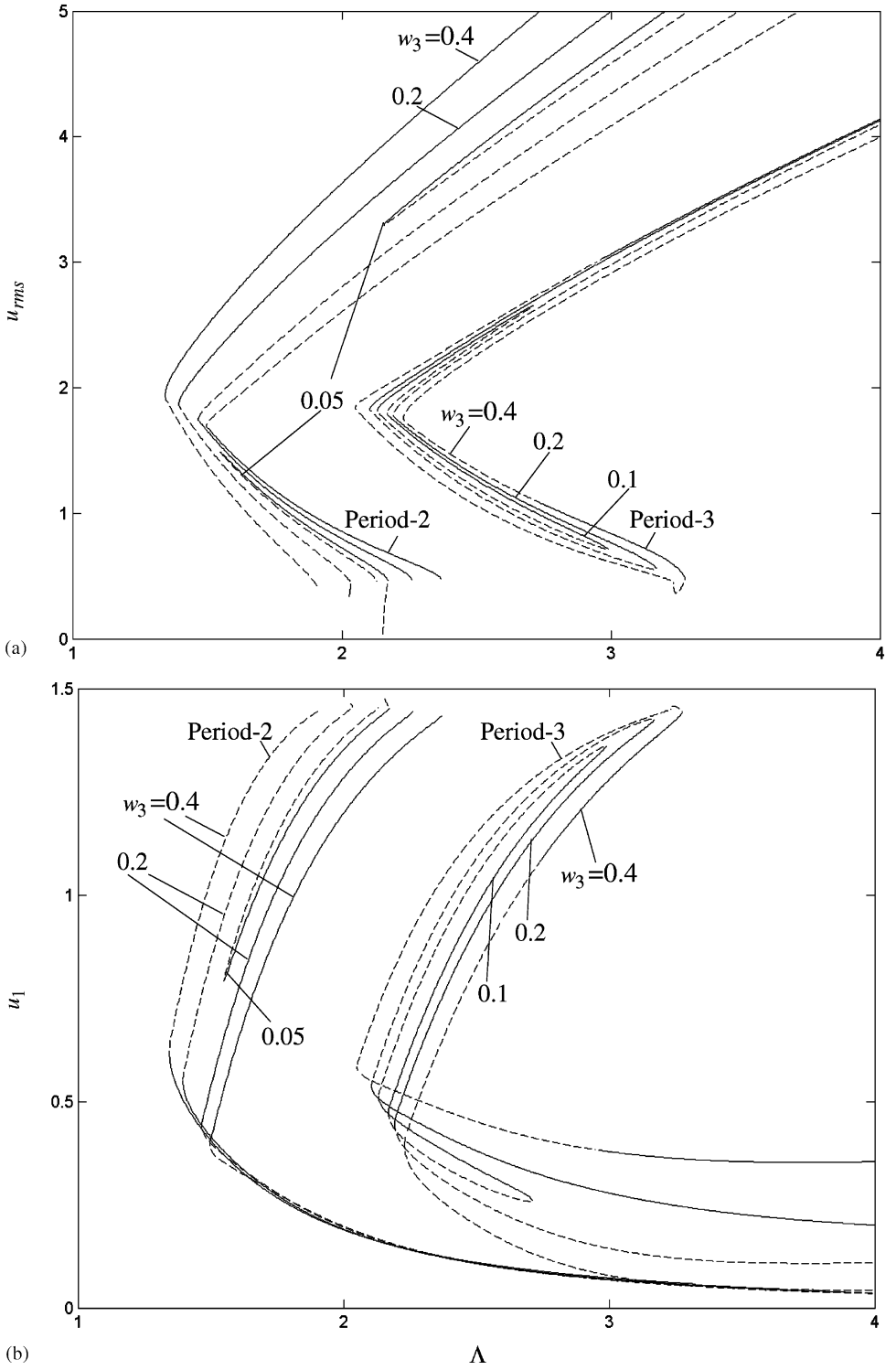

Fig. 5. Influence of w_3 on u_{rms} of an oscillator with $\alpha_1 = 1$, $\alpha_2 = 0$, and $\alpha_3 = 0.2$, given $\zeta = 0.01$, $f_1 = 0.5$, $f_i = 0$ ($i \geqslant 2$), $w_i = 0$ ($i \geqslant 2$ and $i \neq 3$): (a) u_{rms} and (b) u_1 values of period-2 and period-3 motions. (—) Stable and (– –) unstable HBM solutions.

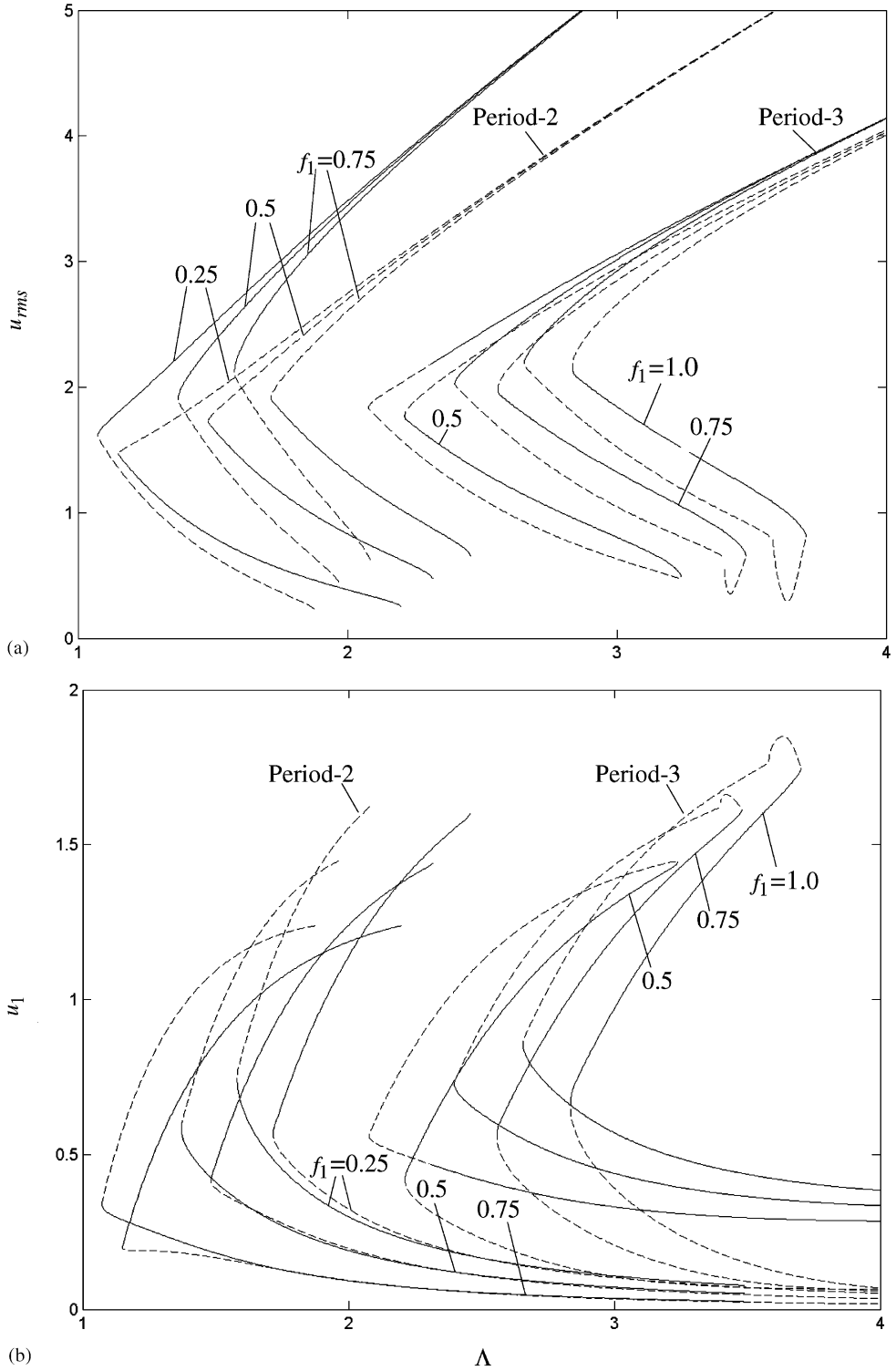

Fig. 6. Influence of f_1 on u_{rms} of an oscillator with $\alpha_1 = 1$, $\alpha_2 = 0$, and $\alpha_3 = 0.2$, given $\zeta = 0.01$, $f_i = 0$ ($i \geqslant 2$), $w_3 = 0.3$: (a) u_{rms} and (b) u_1 values of period-2 and period-3 motions. (—) Stable and (– –) unstable HBM solutions.

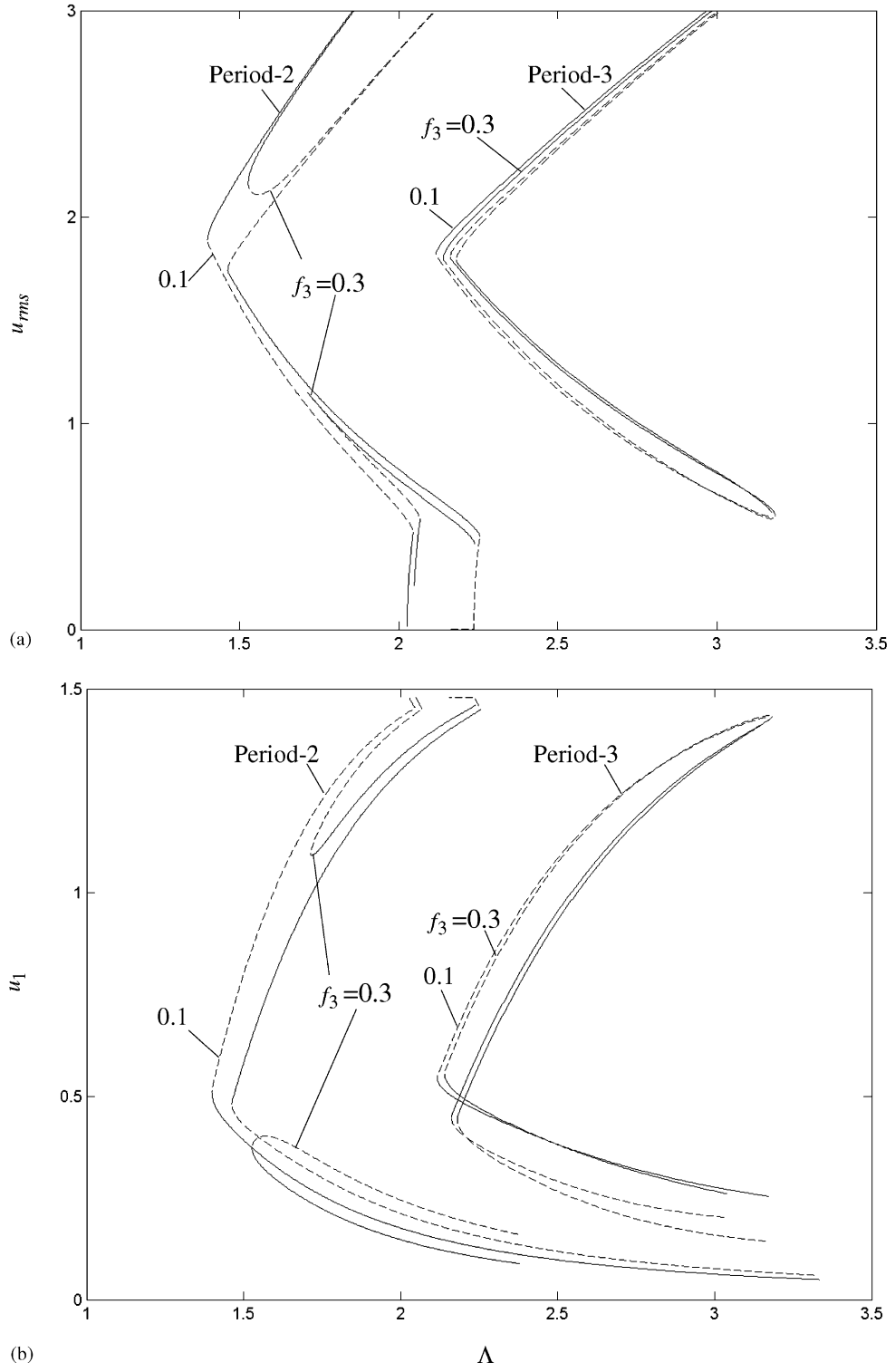

Fig. 7. Influence of f_3 on u_{rms} of an oscillator with $\alpha_1 = 1$, $\alpha_2 = 0$, and $\alpha_3 = 0.2$, given $\zeta = 0.01$, $f_i = 0$ ($i \geqslant 4$), $w_3 = 0.2$: (a) u_{rms} and (b) u_1 values of period-2 and period-3 motions. (—) Stable and (– –) unstable HBM solutions.

SSI and DSI motions are present for the same system when $\zeta \leqslant 0.05$. Within a boundary defined by the response curve for $\zeta = 0.005$, increasing ζ makes the response curve shrink towards the middle. Further increasing ζ, first the DSI motions disappear, followed by the SSI motions. Like the hardening cases in Fig. 3, there is an unstable portion at the beginning of the upper DSI branch. Increasing ζ reduces the frequency range of this unstable DSI section.

Fig. 5 shows the effect of $w(\tau)$ on period-2 and period-3 motions of the same PN systems for $\alpha_3 = 0.2$. A purely harmonic form of $w(\tau)$ is considered in this section. Therefore, only the value of w_3 is varied and other Fourier components w_i of $w(\tau)$ are assumed zero. For period-2 motions, decreasing w_3 has a similar effect as increasing ζ, both of which tend to reduce the u_{rms} amplitude of parametric resonance. The system response u_{rms} changes gradually with w_3, since small changes in w_3 do not result in drastic variations in period-2 and period-3 motions. As the value of w_3 is reduced, stable and unstable SSI branches come closer, and period-2 motions disappear altogether with further reductions in w_3. Finally, a portion of the SSI branch of period-3 motions becomes unstable when $w_3 = 0.4$. This suggests that even though a larger w_3 increases the amplitudes of subharmonic response, stable period-η motions may yield to higher-order subharmonic motions through period-doubling bifurcations [6].

The effect of mean load f_1 on period-2 and period-3 motions of PN systems with cubic nonlinearity is illustrated in Fig. 6. Here, a hardening type PN oscillator with $\alpha_3 = 0.2$ and $\alpha_2 = 0$ is studied for different f_1 values. In this case, the influence of f_1 is again gradual. For both period-2 and period-3 motions, the parametric resonance peaks and the saddle-node bifurcation points connecting SSI and DSI motions are moved to the right on the scale of Λ by increasing f_1. At the same time, the amplitudes of stable SSI motions are increased significantly, while the amplitudes of DSI motions are decreased slightly. Therefore, the influence of f_1 on large-amplitude DSI motions is quite insignificant. In addition, unstable motions exist in the portion of the stable DSI branch of period-3 motions when f_1 is relatively low, as in the case for $f_1 = 0.25$ and 0.5 in Fig. 6. In summary, f_1 also has a significant influence on both period-2 and period-3 motions.

The effect of external excitation $f(\tau)$ on period-2 and period-3 motions of a PN system is illustrated in Fig. 7 with $\alpha_2 = 0$ and $\alpha_3 = 0.2$. A harmonic external force defined by f_3 is considered in addition to a parametric excitation of $w_3 = 0.2$. As demonstrated, an increase of f_3 tends to diminish subharmonic resonances that are excited primarily by w_3. This is because w_3 and f_3 are defined in positive numbers so that $w(\tau)$ and $f(\tau)$ are in phase. The same type of cancellation of in-phase internal and external excitations was exhibited for the period-1 motions as well [1]. When internal and external excitations are out of phase, subharmonic resonances are increased by external excitation amplitude f_3.

4. Conclusions

In this study, the dynamic response of a PN oscillator is investigated near the parametric resonant frequencies. This oscillator is subjected to a mean load and combined parametric and external excitations, as well as a restoring function $g[u(\tau)]$ formed by clearance and continuous nonlinearities. Multiterm HBM is used in conjunction with the Newton–Raphson method and DFT to predict period-η ($\eta = 2, 3$) subharmonic motions. The stability analysis of steady-state response is performed by applying Floquet theory. The HBM predictions of period-1, period-2, and period-3 motions are shown to agree well with the direct numerical integration solutions. A parametric study on the influence of α_3, ζ, w_i, and f_i on period-2 and period-3 subharmonic motions is also included. It is shown that continuous nonlinearities influence the system behavior near parametric resonant frequencies significantly. The unstable DSI motions of period-3 type diminish as ζ or f_1 increase, or $w(\tau)$ decreases. In general, the results of this analysis show that subharmonic motions are very sensitive to the values of three key parameters: damping ratio ζ, time-varying stiffness $w(\tau)$, and mean load f_1. Parametric resonant peaks become extremely significant for very lightly damped systems excited heavily by $w(\tau)$. Parametric resonances are eliminated for large f_1 when the nonlinearity is of the softening type, while the amplitudes of SSI motions are increased for hardening type PN systems. Finally, an external excitation $f(\tau)$ that is in phase with $w(\tau)$ tends to reduce the subharmonic resonance of the steady-state response.

References

[1] Q. Ma, A. Kahraman, Period-one motions of a mechanical oscillator with periodically time-varying, piecewise-nonlinear stiffness, *Journal of Sound and Vibration* 284 (2005) 893–914.
[2] Y.S. Choi, S.T. Noah, Forced periodic vibration of unsymmetric piecewise-linear system, *Journal of Sound and Vibration* 121 (1988) 117–126.
[3] H.S. Choi, J.Y.K. Lou, Nonlinear behavior and chaotic motions of an SDOF system with piecewise-non-linear stiffness, *International Journal of Non-Linear Mechanics* 26 (1991) 461–473.
[4] A. Kahraman, G.W. Blankenship, Experiments on nonlinear dynamic behavior of an oscillator with clearance and periodically time-varying parameters, *Journal of Applied Mechanics* 64 (1997) 217–226.
[5] A. Kahraman, G.W. Blankenship, Interactions between commensurate parametric and forcing excitations in a system with clearance, *Journal of Sound and Vibration* 194 (1996) 317–336.
[6] A. Al-shyyab, A. Kahraman, Non-linear dynamic analysis of a multi-mesh gear train using multi-term harmonic balance method: sub-harmonic motions, *Journal of Sound and Vibration* 279 (2005) 417–451.
[7] A. Kahraman, G.W. Blankenship, Effect of involute contact ratio on spur gear dynamics, *Journal of Mechanical Design* 121 (1999) 111–118.
[8] Q. Ma, A Study of Dynamic Behavior of Piecewise Nonlinear Oscillators with Time-varying Stiffness, Ph.D. Dissertation, The Ohio State University, 2005.